

Relativistic electron-impact ionization of hydrogen atom from its metastable 2S-state in the symmetric/asymmetric coplanar geometries

M. Jakha,¹ S. Mouslih,^{2,1} S. Taj,¹ and B. Manaut^{1,*}

¹*Université Sultan Moulay Slimane, Faculté Polydisciplinaire,
Équipe de Recherche en Physique Théorique et
Matériaux (ERPTM), Béni Mellal, 23000, Morocco.*

²*Faculté des Sciences et Techniques, Laboratoire de Physique
des Matériaux (LPM), Béni Mellal, 23000, Morocco.*

(Dated: December 9, 2021)

Abstract

We analytically compute, in the first Born approximation for symmetric and asymmetric coplanar geometries, the triple differential cross sections for electron-impact ionization of hydrogen atom in the metastable 2S-state at both low and high energies. The process is investigated by using the relativistic Dirac-formalism and it is also shown that the nonrelativistic limit is accurately reproduced when using low incident kinetic energies. At high energies, relativistic and spin effects significantly affect the triple differential cross sections. Our analytical approach which seems exact is compared to some other results in the nonrelativistic regime for asymmetric coplanar geometry. For this particular process and in the absence of any experimental data and theoretical models at high energies, we are not in a position to validate our model. We hope that the present study will provide significant contribution to future experiments.

Keywords : Relativistic ionization ; Relativistic Coulomb wave functions ; Analytical calculations of integrals.

I. INTRODUCTION

Electron-impact ionization is the removal of one or more electrons from the target resulting from the collision between it and an electron. We can distinguish different types of ionization; single ionization, called (e, 2e) process, which occurs when the resulting ion leaves the collision region with a single positive charge, multiple ionization where several electrons in the electronic cortege are ejected and the ion can have multiple positive charges. In this work, however, we will only deal with the case of single ionization of the hydrogen atom from its metastable 2S-state, when is bombarded by an electron of energy E_i greater than the ionization potential. In the collision zone, two electrons emerge with energies E_f and E_B . Even though these two electrons cannot be distinguished, it is convenient to call the faster electron "scattered electron" and the slower one "ejected electron". All ionization reactions are studied in two geometric frameworks. The first is called asymmetric geometry and the second is symmetric geometry, and each of them may be coplanar or noncoplanar. In asymmetric geometries, a fast electron of energy E_i is incident on the target atom, and a fast scattered electron is detected in coincidence with a slow ejected electron. This kind of experiment was first performed by Ehrhardt *et al.* [1]. Symmetric geometries, which

* b.manaut@usms.ma

are defined by the requirement that the two outgoing electrons are detected with the same energies and equal scattering and ejection angles (i.e. $E_f \simeq E_B$ and $\theta_f \simeq \theta_B$), was introduced by Amaldi *et al.* [2]. In coplanar geometry, the three momenta \mathbf{p}_i , \mathbf{p}_f and \mathbf{p}_B are in the same plane, whereas in noncoplanar geometry the momentum \mathbf{p}_B is out of the $(\mathbf{p}_i, \mathbf{p}_f)$ reference plane. Electron-impact ionization of atomic, ionic or molecular systems is one of the important processes of collisional physics, in particular for the study of the structure of matter. It also finds its application in various fields such as astrophysics and plasma physics. Especially, the electron-impact single ionization has proved to be a powerful tool for studying the structure of atoms and their dynamics. Ionization of hydrogen atoms by electron impact is the fundamental and simplest ionization process. The hydrogen atom is an ideal target due to its analytically known wave functions, although it is a particularly difficult target for experimentalists. At present, there are many theoretical models to compute the cross sections of hydrogen-atoms ionization in both the ground and metastable states at various incident kinetic energies and under different kinematic conditions. Unfortunately, ionization from metastable states has not been investigated to the same extent, especially in the relativistic regime, as ionization from the ground state; and this is mainly due to the lack of any experimental studies on this type of ionization. The investigation of the ionization from metastable states of hydrogen atoms by charged particles is now equally interesting and experimental results will soon be available in this field. In particular, the fully triple differential cross sections (TDCS) for the (e, 2e) process have been extensively studied for the ground state hydrogen atom both theoretically and experimentally, while for the ionization from the metastable state no such measurement of TDCS is yet available in the literature, although the absolute total cross sections have been measured much earlier [3, 4]. However, on the theoretical side, quite a few calculations have been performed on the TDCS of the metastable (2S) hydrogen atom using electron impact [5–11] and significant differences were observed in the TDCS structures when compared to the cross section of ground-state ionization. All these theoretical calculations available in the literature to date have been done within the framework of the asymmetric geometry and at low energies. To the best of our knowledge, there is no study available to the ionization of the hydrogen atom from its metastable 2S-state using relativistic formalism at high energies. This work addresses, for the first time, a theoretical study and an analytical calculation of the ionization of the hydrogen atom from its metastable 2S-state at high energies in both symmetric and asymmetric coplanar geometries taking into account the effects of spin and relativity. In the asymmetric coplanar geometry, we present a theoretical semirelativistic Coulomb Born approximation (SRCBA) for the description

of the ionization of hydrogen atom by electron impact in the first Born approximation. In this approximation, the incident and scattered electrons are described by Dirac plane relativistic wave functions while the ejected electron is described by a Sommerfeld-Maue semirelativistic Coulomb wave function and the hydrogen atom, in its metastable state, is described by Darwin's semirelativistic wave function. The TDCS obtained in SRCBA will be compared with the corresponding one in the nonrelativistic Coulomb Born approximation (NRCBA). In the symmetric coplanar geometry, we present the relativistic formalism of the (e, 2e) reaction in the relativistic plane wave Born approximation (RPWBA), where the incident, scattered and ejected electrons are described by relativistic plane waves, and the hydrogen atom in its metastable 2S-state is described by the relativistic exact function, and it will be compared, in the nonrelativistic domain, with the nonrelativistic plane wave Born approximation (NRPWBA). We have found that the relativistic and spin effects, become more and more important by increasing the energy of the incident electron. All the appropriate numerical tests to verify the validity of the analytical results we found were performed with a very good degree of accuracy. The paper is constructed as follows. In section 2, we deliver the different theoretical models in the asymmetric and symmetric coplanar geometries and give, for each model, a detailed account of the techniques which we have used to evaluate the TDCS. In section 3, we discuss the numerical results we have obtained in each geometry. Finally, section 4 is devoted to the conclusions. Atomic units $\hbar = m = e = 1$ are used throughout this work.

II. THEORETICAL MODELS

Let us consider a collision between a hydrogen atom in its metastable 2S-state and an incident electron moving along the z -axis. As a result of this collision, the hydrogen atom becomes ionized and the projectile electron changes its four-momentum from p_i to p_f . In the final state, two electrons (scattered and ejected) emerge with four-momenta p_f and p_B . This reaction can be described, symbolically, as follows:

$$e^-(p_i) + H(2S) \longrightarrow H^+ + e^-(p_B) + e^-(p_f). \quad (1)$$

During this work, we will study the process (1) under two different geometries. We will start first with asymmetric coplanar geometry and then secondly with symmetric coplanar geometry. The detailed calculation of each TDCS in each geometry will be presented.

A. Asymmetric coplanar geometry

We remember that in the case of the Ehrhardt coplanar asymmetric geometry, a fast electron of kinetic energy T_i is incident on the hydrogen target, and a fast scattered electron of kinetic energy T_f is detected in coincidence with a slow ejected electron of kinetic energy T_B . Additionally, the three momenta \mathbf{p}_i , \mathbf{p}_f , and \mathbf{p}_B are in the same plane and the scattering angle θ_f of the scattered electron is fixed and small, while the angle θ_B of the ejected electron is varied. In this geometry, we calculate step by step the exact analytical expression of the semirelativistic spin-unpolarized TDCS in the SRCBA approximation corresponding to the electron-impact ionization of atomic hydrogen in its metastable 2S-state.

1. The S-matrix element

We begin with the first Born ionization S-matrix element for the process (1) in the direct channel in which the exchange effects are neglected. It can be written as

$$\begin{aligned} S_{fi} &= -\frac{i}{c} \int_{-\infty}^{+\infty} dx^0 \langle \psi_{p_f}(x_1) \phi_f(x_2) | V_d | \psi_{p_i}(x_1) \phi_i(x_2) \rangle, \\ &= -i \int_{-\infty}^{+\infty} dt \int d\mathbf{r}_1 \psi_{p_f}^\dagger(t, \mathbf{r}_1) \psi_{p_i}(t, \mathbf{r}_1) \langle \phi_f(x_2) | V_d | \phi_i(x_2) \rangle. \end{aligned} \quad (2)$$

Here, the potential $V_d = 1/r_{12} - 1/r_1$ presents the direct interaction between the incident electron and the hydrogen atom, where $r_{12} = |\mathbf{r}_1 - \mathbf{r}_2|$ and $r_1 = |\mathbf{r}_1|$. The nucleus of the target atom, which is assumed to be infinitely massive, is chosen to be the origin of the coordinate system. The coordinates of the incident and atomic electrons are labeled by \mathbf{r}_1 and \mathbf{r}_2 , respectively. ψ_{p_i} and ψ_{p_f} are the wave functions describing, respectively, the incident and scattered electrons given by a free Dirac solution normalized to the volume V

$$\begin{aligned} \psi_{p_i}(x_1) &= \frac{u(p_i, s_i)}{\sqrt{2E_i V}} e^{-ip_i \cdot x_1}, \\ \psi_{p_f}(x_1) &= \frac{u(p_f, s_f)}{\sqrt{2E_f V}} e^{-ip_f \cdot x_1}, \end{aligned} \quad (3)$$

where E_i and E_f are, respectively, the total energies of the incident and scattered electrons. $\phi_i(x_2) = \phi_i(t, \mathbf{r}_2)$ is the semirelativistic Darwin wave function of atomic hydrogen in its metastable 2S-state, which is accurate to the order Z/c in the relativistic corrections. It is given by

$$\phi_i(t, \mathbf{r}_2) = \exp[-i\mathcal{E}_b(2S)t] \varphi_{2S}^{(\pm)}(\mathbf{r}_2), \quad (4)$$

where $\mathcal{E}_b(2S)$ is the binding energy of the metastable 2S-state of atomic hydrogen given by

$$\mathcal{E}_b(2S) = \frac{c^2}{\sqrt{2}} \sqrt{1 + \sqrt{1 - \alpha^2}} - c^2, \quad (5)$$

where $\alpha = 1/c$ is the fine structure constant. For spin up, $\varphi_{2S}^{(+)}(\mathbf{r}_2)$ is expressed by

$$\varphi_{2S}^{(+)}(\mathbf{r}_2) = N_{D_2} \begin{pmatrix} 2 - r_2 \\ 0 \\ \frac{i(4-r_2)}{4c} \cos(\theta) \\ \frac{i(4-r_2)}{4c} \sin(\theta) e^{i\phi} \end{pmatrix} \frac{1}{4\sqrt{2\pi}} e^{-r_2/2}, \quad (6)$$

where θ and ϕ are the spherical coordinates of \mathbf{r}_2 and

$$N_{D_2} = \frac{4c}{\sqrt{32c^2 + 10}} \quad (7)$$

is the normalization constant. The wave function $\phi_f(x_2) = \phi_f(t, \mathbf{r}_2)$ in Eq. (2) is the Sommerfeld-Maue wave function for continuum states [12], also accurate to the order Z/c in the relativistic corrections. We have

$$\phi_f(t, \mathbf{r}_2) = e^{-iE_B t} \psi_{p_B}^{(-)}(\mathbf{r}_2), \quad (8)$$

where $\psi_{p_B}^{(-)}(\mathbf{r}_2)$ is given, in its final compact form normalized to the volume V , by

$$\begin{aligned} \psi_{p_B}^{(-)}(\mathbf{r}_2) = e^{\pi\eta_B/2} \Gamma(1 + i\eta_B) e^{i\mathbf{p}_B \cdot \mathbf{r}_2} & \left\{ {}_1F_1(-i\eta_B, 1, -i(p_B r_2 + \mathbf{p}_B \cdot \mathbf{r}_2)) + \frac{i}{2cp_B} (\alpha \cdot \mathbf{p}_B + p_B \alpha \cdot \hat{\mathbf{r}}_2) \right. \\ & \left. {}_1F_1(-i\eta_B + 1, 2, -i(p_B r_2 + \mathbf{p}_B \cdot \mathbf{r}_2)) \right\} \frac{u(p_B, s_B)}{\sqrt{2E_B V}}. \end{aligned} \quad (9)$$

η_B is the Sommerfeld parameter given by

$$\eta_B = \frac{E_B}{c^2 p_B}, \quad (10)$$

where E_B is the total energy of the ejected electron and $p_B = |\mathbf{p}_B|$ is the norm of the ejected electron momentum. In Eq. (9), the operator $[\alpha \cdot \mathbf{p}_B]$ acts on the free spinor $u(p_B, s_B)$ and the operator $[\alpha \cdot \hat{\mathbf{r}}_2]$ acts on the spinor part of the Darwin wave function.

The integral over the time coordinate in Eq. (2) can be separated yielding

$$\int dt \exp[i(E_f + E_B - E_i - \mathcal{E}_b(2S))t] = 2\pi \delta(E_f + E_B - E_i - \mathcal{E}_b(2S)), \quad (11)$$

while the integration over $d\mathbf{r}_1$ can be performed by using the well-known following Bethe integral

$$\int d\mathbf{r}_1 e^{i(\mathbf{p}_i - \mathbf{p}_f) \cdot \mathbf{r}_1} \left(\frac{1}{r_{12}} - \frac{1}{r_1} \right) = \frac{4\pi}{\Delta^2} (e^{i\Delta \cdot \mathbf{r}_2} - 1), \quad (12)$$

where the quantity $\Delta = \mathbf{p}_i - \mathbf{p}_f$ is the momentum transfer.

The direct S-matrix element in Eq. (2) becomes

$$\begin{aligned}
S_{fi} = & -i \int d\mathbf{r}_2 \frac{\bar{u}(p_f, s_f)}{\sqrt{2E_f V}} \gamma^0 \frac{u(p_i, s_i)}{\sqrt{2E_i V}} \left\{ {}_1F_1(i\eta_B, 1, i(p_B r_2 + \mathbf{p}_B \cdot \mathbf{r}_2)) - \frac{i}{2cp_B} (\alpha \cdot \mathbf{p}_B \right. \\
& + p_B \alpha \cdot \hat{\mathbf{r}}_2) {}_1F_1(i\eta_B + 1, 2, i(p_B r_2 + \mathbf{p}_B \cdot \mathbf{r}_2)) \left. \right\} \frac{\bar{u}(p_B, s_B) \gamma^0}{\sqrt{2E_B V}} \varphi_{2S}^{(+)}(\mathbf{r}_2) e^{-i\mathbf{p}_B \cdot \mathbf{r}_2} (e^{i\Delta \cdot \mathbf{r}_2} - 1) \\
& \times \frac{8\pi^2}{\Delta^2} \delta(E_f + E_B - E_i - \mathcal{E}_b(2S)) e^{\pi\eta_B/2} \Gamma(1 - i\eta_B).
\end{aligned} \tag{13}$$

This S-matrix element contains two terms $S_{fi}^{(1)}, S_{fi}^{(2)}$. The first one is given by

$$\begin{aligned}
S_{fi}^{(1)} = & -i \int d\mathbf{r}_2 \frac{\bar{u}(p_f, s_f)}{\sqrt{2E_f V}} \gamma^0 \frac{u(p_i, s_i)}{\sqrt{2E_i V}} \frac{\bar{u}(p_B, s_B) \gamma^0}{\sqrt{2E_B V}} \left\{ {}_1F_1(i\eta_B, 1, i(p_B r_2 + \mathbf{p}_B \cdot \mathbf{r}_2)) \right\} \varphi_{2S}^{(+)}(\mathbf{r}_2) \\
& \times e^{-i\mathbf{p}_B \cdot \mathbf{r}_2} (e^{i\Delta \cdot \mathbf{r}_2} - 1) \frac{8\pi^2}{\Delta^2} \delta(E_f + E_B - E_i - \mathcal{E}_b(2S)) e^{\pi\eta_B/2} \Gamma(1 - i\eta_B).
\end{aligned} \tag{14}$$

This first term can be reformulated in the following form

$$\begin{aligned}
S_{fi}^{(1)} = & -i [H_1(\mathbf{q} = \Delta - \mathbf{p}_B) - H_1(\mathbf{q} = -\mathbf{p}_B)] \frac{\bar{u}(p_f, s_f)}{\sqrt{2E_f V}} \gamma^0 \frac{u(p_i, s_i)}{\sqrt{2E_i V}} \frac{\bar{u}(p_B, s_B) \gamma^0}{\sqrt{2E_B V}} \\
& \times \frac{8\pi^2}{\Delta^2} \delta(E_f + E_B - E_i - \mathcal{E}_b(2S)) e^{\pi\eta_B/2} \Gamma(1 - i\eta_B),
\end{aligned} \tag{15}$$

where $H_1(\mathbf{q})$ is given by

$$H_1(\mathbf{q}) = \int d\mathbf{r}_2 e^{i\mathbf{q} \cdot \mathbf{r}_2} {}_1F_1(i\eta_B, 1, i(p_B r_2 + \mathbf{p}_B \cdot \mathbf{r}_2)) \varphi_{2S}^{(+)}(\mathbf{r}_2). \tag{16}$$

According to the expression of $\varphi_{2S}^{(+)}(\mathbf{r}_2)$ given in Eq. (6), $H_1(\mathbf{q})$ can be written as

$$H_1(\mathbf{q}) = \frac{N_{D_2}}{4\sqrt{2\pi}} (I_1, 0, I_2, I_3)^T, \tag{17}$$

and one has to evaluate

$$I_1 = \int d\mathbf{r}_2 (2 - r_2) e^{-r_2/2} e^{i\mathbf{q} \cdot \mathbf{r}_2} {}_1F_1(i\eta_B, 1, i(p_B r_2 + \mathbf{p}_B \cdot \mathbf{r}_2)). \tag{18}$$

In this integral, we are confronted with the task of evaluating two types of integrals, one of which is

$$I'_1 = 2 \int d\mathbf{r}_2 e^{-r_2/2} e^{i\mathbf{q} \cdot \mathbf{r}_2} {}_1F_1(i\eta_B, 1, i(p_B r_2 + \mathbf{p}_B \cdot \mathbf{r}_2)), \tag{19}$$

and the other one is

$$I''_1 = \int d\mathbf{r}_2 r_2 e^{-r_2/2} e^{i\mathbf{q} \cdot \mathbf{r}_2} {}_1F_1(i\eta_B, 1, i(p_B r_2 + \mathbf{p}_B \cdot \mathbf{r}_2)). \tag{20}$$

In order to evaluate the first integral I'_1 , we take recourse to the well-known integral [13]

$$\begin{aligned} I(\lambda) &= \int d\mathbf{r} e^{i\mathbf{q}\cdot\mathbf{r}} \frac{e^{-\lambda r}}{r} {}_1F_1(i\eta_B, 1, i(p_B r_2 + \mathbf{p}_B \cdot \mathbf{r}_2)), \\ &= \frac{4\pi}{q^2 + \lambda^2} \exp \left[i\eta_B \ln \left(\frac{q^2 + \lambda^2}{q^2 + \lambda^2 + 2\mathbf{q} \cdot \mathbf{p}_B - 2i\lambda p_B} \right) \right], \end{aligned} \quad (21)$$

where λ is a real variable. Then, the integral I'_1 reads

$$I'_1 = 2 \left(- \frac{\partial I(\lambda)}{\partial \lambda} \right) \Big|_{\lambda=1/2}. \quad (22)$$

For the integral I''_1 , there are two methods to perform it. The first one is by using the integral $I(\lambda)$ (21). This yields

$$I''_1 = \left(\frac{\partial^2 I(\lambda)}{\partial \lambda^2} \right) \Big|_{\lambda=1/2}. \quad (23)$$

The second method that we prefer to use here is through the direct application of an analytical formula given by Gravielle in [14]

$$I''_1 = \frac{8\pi}{D^3} A_1^{-i\eta_B} \left[L_{10} + L_{11} \frac{1}{A_1} + L_{12} \frac{1}{A_1^2} \right] \Big|_{\lambda=1/2}, \quad (24)$$

where

$$\begin{aligned} D &= \lambda^2 + q^2, \quad A_1 = 1 - \frac{2(\mathbf{q} \cdot \mathbf{p}_B + i\lambda p_B)}{D}, \\ L_{10} &= (1 - i\eta_B)[2(2 - i\eta_B)\lambda^2 - D], \\ L_{11} &= i\eta_B[4\lambda(1 - i\eta_B)(\lambda - ip_B) - D], \\ L_{12} &= 2i\eta_B(1 + i\eta_B)(\lambda - ip_B)^2. \end{aligned} \quad (25)$$

The other integrals I_2 and I_3 in (17) can be obtained by noting that

$$\cos(\theta) e^{i\mathbf{q} \cdot \mathbf{r}_2} = -\frac{i}{r_2} \frac{\partial}{\partial q_z} e^{i\mathbf{q} \cdot \mathbf{r}_2}, \quad (26)$$

and

$$\sin(\theta) e^{i\phi} e^{i\mathbf{q} \cdot \mathbf{r}_2} = -\frac{i}{r_2} \left(\frac{\partial}{\partial q_x} + i \frac{\partial}{\partial q_y} \right) e^{i\mathbf{q} \cdot \mathbf{r}_2}. \quad (27)$$

Thus we finally get

$$\begin{aligned} I_2 &= \frac{1}{c} \frac{\partial}{\partial q_z} \left[I(\lambda) + \frac{1}{4} \frac{\partial I(\lambda)}{\partial \lambda} \right] \Big|_{\lambda=1/2}, \\ I_3 &= \frac{1}{c} \left[\frac{\partial}{\partial q_x} + i \frac{\partial}{\partial q_y} \right] \left[I(\lambda) + \frac{1}{4} \frac{\partial I(\lambda)}{\partial \lambda} \right] \Big|_{\lambda=1/2}. \end{aligned} \quad (28)$$

The second term in the S-matrix element given in Eq. (13) is

$$S_{fi}^{(2)} = S_{fi}^{(2),1} + S_{fi}^{(2),2}, \quad (29)$$

with

$$\begin{aligned} S_{fi}^{(2),1} = & - \int d\mathbf{r}_2 \frac{\bar{u}(p_f, s_f)}{\sqrt{2E_f V}} \gamma^0 \frac{u(p_i, s_i)}{\sqrt{2E_i V}} \frac{1}{2cp_B} \frac{\bar{u}(p_B, s_B) \gamma^0}{\sqrt{2E_B V}} \left[\gamma^0 \frac{E_B}{c} - \not{p}_B \right] \varphi_{2S}^{(+)}(\mathbf{r}_2) \\ & \times {}_1F_1(i\eta_B + 1, 2, i(p_B r_2 + \mathbf{p}_B \cdot \mathbf{r}_2)) e^{-i\mathbf{p}_B \cdot \mathbf{r}_2} (e^{i\mathbf{\Delta} \cdot \mathbf{r}_2} - 1) \\ & \times \frac{8\pi^2}{\Delta^2} \delta(E_f + E_B - E_i - \mathcal{E}_b(2S)) e^{\pi\eta_B/2} \Gamma(1 - i\eta_B), \end{aligned} \quad (30)$$

and

$$\begin{aligned} S_{fi}^{(2),2} = & - \int d\mathbf{r}_2 \frac{\bar{u}(p_f, s_f)}{\sqrt{2E_f V}} \gamma^0 \frac{u(p_i, s_i)}{\sqrt{2E_i V}} \frac{1}{2c} \frac{\bar{u}(p_B, s_B) \gamma^0}{\sqrt{2E_B V}} \varphi_{2S}^{'(+)}(\mathbf{r}_2) {}_1F_1(i\eta_B + 1, 2, i(p_B r_2 + \mathbf{p}_B \cdot \mathbf{r}_2)) \\ & \times e^{-i\mathbf{p}_B \cdot \mathbf{r}_2} (e^{i\mathbf{\Delta} \cdot \mathbf{r}_2} - 1) \frac{8\pi^2}{\Delta^2} \delta(E_f + E_B - E_i - \mathcal{E}_b(2S)) e^{\pi\eta_B/2} \Gamma(1 - i\eta_B). \end{aligned} \quad (31)$$

The operator $[\alpha \cdot \mathbf{p}_B]$ in Eq. (30) is replaced by $[\gamma^0 \frac{E_B}{c} - \not{p}_B]$, and in Eq. (31) $\varphi_{2S}^{'(+)}(\mathbf{r}_2)$ is given by

$$\varphi_{2S}^{'(+)}(\mathbf{r}_2) = [\alpha \cdot \hat{\mathbf{r}}_2] \varphi_{2S}^{(+)}(\mathbf{r}_2) = \frac{N_{D_2}}{4\sqrt{2\pi}} e^{-r_2/2} \begin{pmatrix} \frac{i(4-r_2)}{4c} \\ 0 \\ (2-r_2) \cos(\theta) \\ (2-r_2) \sin(\theta) e^{i\phi} \end{pmatrix}. \quad (32)$$

$S_{fi}^{(2),1}$ can be recasted in the following form

$$\begin{aligned} S_{fi}^{(2),1} = & - [H_2(\mathbf{q} = \mathbf{\Delta} - \mathbf{p}_B) - H_2(\mathbf{q} = -\mathbf{p}_B)] \frac{\bar{u}(p_f, s_f)}{\sqrt{2E_f V}} \gamma^0 \frac{u(p_i, s_i)}{\sqrt{2E_i V}} \frac{1}{2cp_B} \frac{\bar{u}(p_B, s_B) \gamma^0}{\sqrt{2E_B V}} \\ & \times \left[\gamma^0 \frac{E_B}{c} - \not{p}_B \right] \frac{8\pi^2}{\Delta^2} \delta(E_f + E_B - E_i - \mathcal{E}_b(2S)) e^{\pi\eta_B/2} \Gamma(1 - i\eta_B), \end{aligned} \quad (33)$$

where $H_2(\mathbf{q})$ is the integral expressed by

$$H_2(\mathbf{q}) = \int d\mathbf{r}_2 e^{i\mathbf{q} \cdot \mathbf{r}_2} {}_1F_1(i\eta_B + 1, 2, i(p_B r_2 + \mathbf{p}_B \cdot \mathbf{r}_2)) \varphi_{2S}^{(+)}(\mathbf{r}_2). \quad (34)$$

Replacing the Darwin function in Eq. (34) by its expression (6) leads to

$$H_2(\mathbf{q}) = \frac{N_{D_2}}{4\sqrt{2\pi}} (J_1, 0, J_2, J_3)^T, \quad (35)$$

where

$$\begin{aligned} J_1 = & \int d\mathbf{r}_2 e^{i\mathbf{q} \cdot \mathbf{r}_2} e^{-r_2/2} (2-r_2) {}_1F_1(i\eta_B + 1, 2, i(p_B r_2 + \mathbf{p}_B \cdot \mathbf{r}_2)), \\ J_2 = & \frac{i}{4c} \int d\mathbf{r}_2 e^{i\mathbf{q} \cdot \mathbf{r}_2} e^{-r_2/2} (4-r_2) \cos(\theta) {}_1F_1(i\eta_B + 1, 2, i(p_B r_2 + \mathbf{p}_B \cdot \mathbf{r}_2)), \\ J_3 = & \frac{i}{4c} \int d\mathbf{r}_2 e^{i\mathbf{q} \cdot \mathbf{r}_2} e^{-r_2/2} (4-r_2) \sin(\theta) e^{i\phi} {}_1F_1(i\eta_B + 1, 2, i(p_B r_2 + \mathbf{p}_B \cdot \mathbf{r}_2)). \end{aligned} \quad (36)$$

To evaluate this three integrals, we introduce a new integral that has been calculated analytically by Attaourti *et al* in [15]

$$\begin{aligned} J(\lambda) &= \int d\mathbf{r} e^{i\mathbf{q}\cdot\mathbf{r}} \frac{e^{-\lambda r}}{r} {}_1F_1(i\eta_B + 1, 2, i(p_B r_2 + \mathbf{p}_B \cdot \mathbf{r}_2)), \\ &= \frac{4\pi}{(q^2 + \lambda^2)} {}_2F_1\left(i\eta_B + 1, 1, 2, -2 \frac{(\mathbf{q} \cdot \mathbf{p}_B - i\lambda p_B)}{q^2 + \lambda^2}\right), \end{aligned} \quad (37)$$

where λ is a real variable.

In the same way as before and after some manipulations, one gets

$$\begin{aligned} J_1 &= -2 \left(\frac{\partial J(\lambda)}{\partial \lambda} \right) - \frac{\partial^2 J(\lambda)}{\partial \lambda^2} \Big|_{\lambda=1/2}, \\ J_2 &= \frac{1}{c} \frac{\partial}{\partial q_z} \left[J(\lambda) + \frac{1}{4} \frac{\partial J(\lambda)}{\partial \lambda} \right] \Big|_{\lambda=1/2}, \\ J_3 &= \frac{1}{c} \left[\frac{\partial}{\partial q_x} + i \frac{\partial}{\partial q_y} \right] \left[J(\lambda) + \frac{1}{4} \frac{\partial J(\lambda)}{\partial \lambda} \right] \Big|_{\lambda=1/2}. \end{aligned} \quad (38)$$

For the term $S_{fi}^{(2),2}$, it can be written as

$$\begin{aligned} S_{fi}^{(2),2} &= -[H_3(\mathbf{q} = \mathbf{\Delta} - \mathbf{p}_B) - H_3(\mathbf{q} = -\mathbf{p}_B)] \frac{\bar{u}(p_f, s_f)}{\sqrt{2E_f V}} \gamma^0 \frac{u(p_i, s_i)}{\sqrt{2E_i V}} \frac{1}{2c} \frac{\bar{u}(p_B, s_B) \gamma^0}{\sqrt{2E_B V}} \\ &\times \frac{8\pi^2}{\Delta^2} \delta(E_f + E_B - E_i - \mathcal{E}_b(2S)) e^{\pi\eta_B/2} \Gamma(1 - i\eta_B). \end{aligned} \quad (39)$$

The quantity $H_3(\mathbf{q})$ is given by

$$H_3(\mathbf{q}) = \frac{N_{D_2}}{4\sqrt{2}\pi} (K_1, 0, K_2, K_3)^T, \quad (40)$$

where K_1 , K_2 and K_3 are three integrals whose solutions are

$$\begin{aligned} K_1 &= -\frac{i}{c} \left[\frac{\partial J(\lambda)}{\partial \lambda} + \frac{1}{4} \frac{\partial^2 J(\lambda)}{\partial \lambda^2} \right] \Big|_{\lambda=1/2}, \\ K_2 &= -i \frac{\partial}{\partial q_z} \left[2J(\lambda) + \frac{\partial J(\lambda)}{\partial \lambda} \right] \Big|_{\lambda=1/2}, \\ K_3 &= -i \left[\frac{\partial}{\partial q_x} + i \frac{\partial}{\partial q_y} \right] \left[2J(\lambda) + \frac{\partial J(\lambda)}{\partial \lambda} \right] \Big|_{\lambda=1/2}. \end{aligned} \quad (41)$$

2. Spin-unpolarized TDCS in the SRCBA

Using the standard procedures of QED [16], we obtain for the spin-unpolarized TDCS

$$\frac{d\bar{\sigma}^{(SRCBA)}}{dE_B d\Omega_B d\Omega_f} = \frac{1}{16\pi^3 c^6} \frac{|\mathbf{p}_f| |\mathbf{p}_B|}{|\mathbf{p}_i|} \frac{e^{\pi\eta_B}}{\Delta^4} |\Gamma(1 - i\eta_B)|^2 \left| \widehat{S}_{fi}^{(1)} + \widehat{S}_{fi}^{(2),1} + \widehat{S}_{fi}^{(2),2} \right|^2 \Big|_{E_f = E_i + \mathcal{E}_b(2S) - E_B}, \quad (42)$$

with

$$\widehat{S}_{fi}^{(1)} = \frac{1}{2} \sum_{s_i, s_f} \sum_{s_B} [\bar{u}(p_f, s_f) \gamma^0 u(p_i, s_i)] [\bar{u}(p_B, s_B) \gamma^0] [i(H_1(\mathbf{q} = \mathbf{\Delta} - \mathbf{p}_B) - H_1(\mathbf{q} = -\mathbf{p}_B))], \quad (43)$$

$$\begin{aligned} \widehat{S}_{fi}^{(2),1} &= \frac{1}{2} \sum_{s_i, s_f} \sum_{s_B} [\bar{u}(p_f, s_f) \gamma^0 u(p_i, s_i)] [\bar{u}(p_B, s_B) \gamma^0] \left[\gamma^0 \frac{E_B}{c} - \not{p}_B \right] \frac{1}{2cp_B} \\ &\times [H_2(\mathbf{q} = \mathbf{\Delta} - \mathbf{p}_B) - H_2(\mathbf{q} = -\mathbf{p}_B)], \end{aligned} \quad (44)$$

$$\widehat{S}_{fi}^{(2),2} = \frac{1}{2} \sum_{s_i, s_f} \sum_{s_B} [\bar{u}(p_f, s_f) \gamma^0 u(p_i, s_i)] [\bar{u}(p_B, s_B) \gamma^0] \frac{1}{2c} [H_3(\mathbf{q} = \mathbf{\Delta} - \mathbf{p}_B) - H_3(\mathbf{q} = -\mathbf{p}_B)]. \quad (45)$$

In Eq. (42), $|\mathbf{p}_i|$ and $|\mathbf{p}_f|$ are, respectively, the norms of the initial and final electron momenta. All the calculations in Eq. (42) can be done analytically and only five terms out of nine are nonzero, the diagonal terms $|\widehat{S}_{fi}^{(1)}|^2$, $|\widehat{S}_{fi}^{(2),1}|^2$, $|\widehat{S}_{fi}^{(2),2}|^2$, and $\widehat{S}_{fi}^{(1)\dagger} \widehat{S}_{fi}^{(2),1}$, as well as $\widehat{S}_{fi}^{(2),1\dagger} \widehat{S}_{fi}^{(1)}$. In Eqs. (43)-(45), the different sums over spin states give the following results:

$$\frac{1}{2} \sum_{s_i, s_f} |\bar{u}(p_f, s_f) \gamma^0 u(p_i, s_i)|^2 = 2c^2 \left(\frac{2E_i E_f}{c^2} - (p_i \cdot p_f) + c^2 \right), \quad (46)$$

$$\sum_{s_B} \left| \bar{u}(p_B, s_B) \gamma^0 \left[\gamma^0 \frac{E_B}{c} - \not{p}_B \right] \right|^2 = 4E_B \left(\frac{E_B^2}{c^2} - c^2 \right), \quad (47)$$

$$\sum_{s_B} |\bar{u}(p_B, s_B) \gamma^0|^2 = 4E_B, \quad (48)$$

$$\frac{1}{2} \sum_{s_i} (...) = 1(...), \quad (49)$$

where $(p_i \cdot p_f)$ in Eq. (46) is the scalar product of initial and final four-momentum, and $\sum_{s_i} (...)/2$ denotes the averaged sum over the spin states of the target atomic hydrogen.

We have to compare the TDCS in Eq. (42) with the corresponding one in the Non-Relativistic Coulomb Born Approximation (NRCBA), where the incident and scattered electrons are described by non-relativistic plane waves:

$$\psi_{p_{i,f}}(\mathbf{r}_1) = (2\pi)^{-3/2} e^{i\mathbf{p}_{i,f} \cdot \mathbf{r}_1}, \quad (50)$$

whereas the ejected electron is described by a Coulomb wave function:

$$\psi_{c,p_B}(\mathbf{r}_2) = (2\pi)^{-3/2} e^{i\mathbf{p}_B \cdot \mathbf{r}_2} e^{\pi/2p_B} \Gamma \left(1 + \frac{i}{p_B} \right) {}_1F_1 \left(-\frac{i}{p_B}, 1, -(p_B r_2 + \mathbf{p}_B \cdot \mathbf{r}_2) \right), \quad (51)$$

and the hydrogen atomic in its metastable 2S-state is described by the non-relativistic (NR) wave function [17]

$$\psi_{2S}^{NR}(\mathbf{r}_2) = \frac{1}{4\sqrt{2\pi}} (2 - r_2) e^{-r_2/2}. \quad (52)$$

Thus, the TDCS in the NRCBA is given by:

$$\frac{d\bar{\sigma}^{(NRCBA)}}{dE_B d\Omega_B d\Omega_f} = \frac{p_f p_B}{p_i} |f_{ion}^{CBA}|^2, \quad (53)$$

where f_{ion}^{CBA} is the first Coulomb-Born amplitude corresponding to the ionization of metastable 2S-state hydrogen atom by electron impact which is given by:

$$f_{ion}^{CBA} = -\frac{2}{\Delta^2} \frac{e^{\pi/2 p_B}}{4(2\pi)^2} \Gamma\left(1 - \frac{i}{p_B}\right) \left[-2 \left(\frac{\partial I(\mathbf{q} = \mathbf{\Delta} - \mathbf{p}_B)}{\partial \lambda} - \frac{\partial I(\mathbf{q} = -\mathbf{p}_B)}{\partial \lambda} \right) - (I_1''(\mathbf{q} = \mathbf{\Delta} - \mathbf{p}_B) - I_1''(\mathbf{q} = -\mathbf{p}_B)) \right] \Big|_{\lambda=1/2}, \quad (54)$$

where the integral $I(\mathbf{q})$ is the same as that given previously in Eq. (21), and $I_1''(\mathbf{q})$ is the same integral taken from [Gravielle] (24), but here $\eta_B = 1/p_B$.

B. Symmetric coplanar geometry

The symmetric coplanar geometry can be considered as a particular case of asymmetric coplanar geometry. Let us first remind that the symmetric geometry, also called binary geometry, is defined by the requirement that the kinetic energies of the scattered and ejected electrons are nearly the same, and the scattered and ejected electron angles with respect to the incident beam direction are equal to each other. In this section, we present the relativistic formalism of the $(e, 2e)$ reaction in the Relativistic Plane Wave Born Approximation (RPWBA), where the incident, scattered, and ejected electrons are described by relativistic plane waves, and the hydrogen atom in its metastable 2S-state is described by the relativistic exact function given by:

$$\phi_i(t, \mathbf{r}_2) = \exp[-i\mathcal{E}_b(2S)t] \varphi_{Exact}^{(\pm), 2S}(\mathbf{r}_2), \quad (55)$$

where $\mathcal{E}_b(2S)$ is the binding energy of the metastable 2S-state of atomic hydrogen given in (5). For spin up, $\varphi_{Exact}^{(+), 2S}(\mathbf{r}_2)$ is expressed by:

$$\begin{aligned} \varphi_{Exact}^{(+), 2S}(\mathbf{r}_2) = & \frac{1}{2\sqrt{4\pi}} \frac{(2Z)^{\gamma_H+1/2}}{a_{2S}^{\gamma_H+1}} \sqrt{\frac{2\gamma_H+1}{(a_{2S}+1)\Gamma(2\gamma_H+1)}} r_2^{\gamma_H-1} e^{-Zr_2/a_{2S}} \\ & \times \begin{pmatrix} ig_{2S_{1/2}}(r_2) \\ 0 \\ f_{2S_{1/2}}(r_2) \cos(\theta) \\ f_{2S_{1/2}}(r_2) \sin(\theta) e^{i\phi} \end{pmatrix}, \end{aligned} \quad (56)$$

where θ and ϕ are the spherical coordinates of \mathbf{r}_2 . The two quantities $g_{2S_{1/2}}(r_2)$ and $f_{2S_{1/2}}(r_2)$ are such as:

$$\begin{aligned} g_{2S_{1/2}}(r_2) &= \sqrt{1 + \frac{Z\alpha}{\sqrt{2(1-\gamma_H)}}} \left[\left(1 - \frac{2Zr_2}{a_{2S}(2\gamma_H+1)} \right) (a_{2S}+1) - 1 \right], \\ f_{2S_{1/2}}(r_2) &= \sqrt{1 - \frac{Z\alpha}{\sqrt{2(1-\gamma_H)}}} \left[\left(1 - \frac{2Zr_2}{a_{2S}(2\gamma_H+1)} \right) (a_{2S}+1) + 1 \right], \end{aligned} \quad (57)$$

where Z is the atomic number, and the two parameters γ_H and a_{2S} are given by:

$$\begin{aligned} \gamma_H &= \sqrt{1 - Z^2\alpha^2}, \\ a_{2S} &= \sqrt{2(\gamma_H+1)}, \end{aligned} \quad (58)$$

with $\alpha = 1/c$ is the fine structure constant.

Substituting all these expressions into the first Born S-matrix element (2) and after some manipulations, one gets

$$\begin{aligned} \frac{d\bar{\sigma}^{(RPWBA)}}{dE_B d\Omega_B d\Omega_f} &= \frac{1}{2} \frac{p_f p_B}{c^6 p_i \Delta^4} \left(\frac{1}{2} \sum_{s_i, s_f} |\bar{u}(p_f, s_f) \gamma^0 u(p_i, s_i)|^2 \right) \sum_{s_B} |\bar{u}(p_B, s_B) \gamma^0|^2 \\ &\times |\Phi_{2,1/2,1/2}(\mathbf{q} = \mathbf{\Delta} - \mathbf{p}_B) - \Phi_{2,1/2,1/2}(\mathbf{q} = -\mathbf{p}_B)|^2. \end{aligned} \quad (59)$$

The different sums over spin states s_i , s_f and s_B are given before in Eqs. (46-48). The functions $\Phi_{2,1/2,1/2}(\mathbf{q})$ are the Fourier transforms of the relativistic atomic hydrogen wave functions

$$\Phi_{n=2,j=1/2,m=1/2}(\mathbf{q}) = (2\pi)^{-3/2} \int d\mathbf{r}_2 e^{i\mathbf{q}\cdot\mathbf{r}_2} \varphi_{Exact}^{(+),2S}(\mathbf{r}_2), \quad (60)$$

and $\mathbf{\Delta} = \mathbf{p}_i - \mathbf{p}_f$ is the momentum transfer. Replacing the exact function $\varphi_{Exact}^{(+),2S}(\mathbf{r}_2)$ by its expression (56) yields

$$\begin{aligned} \Phi_{n=2,j=1/2,m=1/2}(\mathbf{q}) &= (2\pi)^{-3/2} \frac{1}{2\sqrt{4\pi}} \frac{(2Z)^{\gamma_H+1/2}}{a_{2S}^{\gamma_H+1}} \sqrt{\frac{2\gamma_H+1}{(a_{2S}+1)\Gamma(2\gamma_H+1)}} \\ &\times \begin{pmatrix} \int d\mathbf{r}_2 e^{i\mathbf{q}\cdot\mathbf{r}_2} r_2^{\gamma_H-1} e^{-Zr_2/a_{2S}} i g_{2S_{1/2}}(r_2) \\ 0 \\ \int d\mathbf{r}_2 e^{i\mathbf{q}\cdot\mathbf{r}_2} r_2^{\gamma_H-1} e^{-Zr_2/a_{2S}} f_{2S_{1/2}}(r_2) \cos(\theta) \\ \int d\mathbf{r}_2 e^{i\mathbf{q}\cdot\mathbf{r}_2} r_2^{\gamma_H-1} e^{-Zr_2/a_{2S}} f_{2S_{1/2}}(r_2) \sin(\theta) e^{i\phi} \end{pmatrix}. \end{aligned} \quad (61)$$

The expression of the TDCS in the Semi-Relativistic Plan Wave Born Approximation (SRPWBA) remains similar to that given in the RPWBA (59), except the expression of the Fourier transform which changes since the wave function describing the hydrogen atom in the SRPWBA is replaced by

the Darwin wave function that we have previously expressed in Eq. (6). This TDCS in Eq. (59) is to be compared with the corresponding one in the Non-Relativistic Plane Wave Born Approximation (NRPWBA), where the incident, scattered, and ejected electrons are described by non-relativistic plane waves:

$$\frac{d\bar{\sigma}^{(NRPWBA)}}{dE_B d\Omega_B d\Omega_f} = \frac{2^{10}}{\pi^2 \Delta^4} \frac{p_f p_B}{p_i} \left[\frac{4\mathbf{q}^2 - 1}{(1 + 4\mathbf{q}^2)^3} - \frac{4\mathbf{q}_0^2 - 1}{(1 + 4\mathbf{q}_0^2)^3} \right]^2, \quad (62)$$

where $\mathbf{q} = \mathbf{\Delta} - \mathbf{p}_B$ and $\mathbf{q}_0 = -\mathbf{p}_B$.

III. RESULTS AND DISCUSSION

In this paper, we develop an exact relativistic model, in the first Born approximation, to study the ionization of the metastable 2S-state hydrogen atom by electrons impact at high energies in the asymmetric and symmetric coplanar geometries. The required derivatives of hypergeometric functions and all integrals resulting from the Fourier transforms of the relativistic and semirelativistic atomic hydrogen wave functions are computed in closed analytic forms using the programming language MATHEMATICA, which is also used to plot the various figures of the present work. In this section, we will present all the numerical results obtained in both asymmetric and symmetric geometries; during that, we will follow the same arrangement that we adopted in the previous section. We will start first with the results obtained in the case of asymmetric geometry and then symmetric geometry. All the TDCSs are given in atomic units.

A. Asymmetric coplanar geometry

We will begin our discussion, in this case, by comparing our results with those obtained by Hafid *et al.* [5] in the nonrelativistic domain. Hafid's results were obtained using the well-known approximation BBK model of Brauner *et al.* [7], and when Hafid presented his results, he also compared with those obtained by Coulomb wave functions and second born calculations of Vucic *et al.* [6] with respect to the incoming electron kinetic energy of 250 eV and the ejected electron kinetic energy of 5 eV. In the following figures (Fig. (1), Fig. (2) and Fig. (3)), which contain the comparison with other theoretical calculations, the angular choice is as follows: p_i is along the z -axis and $\theta_i = 0^\circ, \phi_i = 0^\circ$. For the scattered electron, we choose $\phi_f = 0^\circ$ and θ_f is fixed in Figs. (1) and (2), respectively, to the values $\theta_f = 3^\circ$ and $\theta_f = 5^\circ$, while in Fig. (3) θ_f varies from -12° to 12° . For the ejected electron, we choose $\phi_B = 0^\circ$ and θ_B varies from 0° to 360° in Figs. (1)

and (2) and it is fixed to the value $\theta_B = 20^\circ$ in Fig. (3).

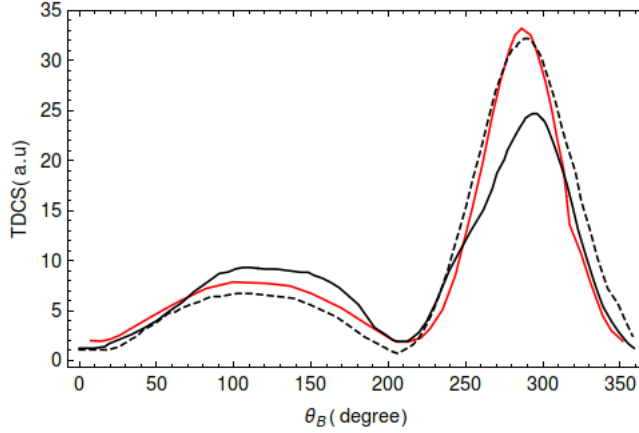


Figure 1: The TDCS of the (e, 2e) ionization of hydrogen 2S in terms of the ejection angle θ_B . The incident and the ejected electron kinetic energies are 250 eV and 5 eV respectively and the scattering angle $\theta_f = 3^\circ$. The solid red line gives our results (NRCBA) given in Eq.(53), the solid black line those of Hafid *et al.* [5] and the dashed line results obtained by Coulomb wave functions.

We compare, in Fig (1), our results in the NRCBA (Eq.(53)) with those of Hafid *et al.* and those obtained by Coulomb wave functions (where the product of two Coulomb wave solutions is used for the scattered and ejected electrons) for the incident kinetic energy of 250 eV, ejection kinetic energy value of 5 eV and the scattering angle of $\theta_f = 3^\circ$. Our results in the NRCBA model were obtained, as we have seen in the theoretical calculations in the previous section, by using a Coulomb wave function to describe only the ejected electron, whereas the fast incident and scattered electrons are described by non-relativistic plane wave functions, thus neglecting the Coulomb interaction of the fast scattered electron with the system. Comparing these results with those of other case in which the scattered and ejected electrons are described together by a Coulomb wave functions, we find that the results are very close, both in the shape of the curve and the location of the peaks, as well as in the order of magnitude. The slight difference between the different approaches, in terms of magnitude, may be due to the Coulomb wave function that was used not only to describe the ejected electron, as we did in our model (NRCBA), but even to describe also the final electron. These two results obtained using the Coulomb wave functions remain different in magnitude, as well as in the height of the binary peak from the result obtained by Hafid *et al.* using BBK approximation. Figure (2) represents similar parameterization as in Fig. (1), but with the scattering angle $\theta_f = 5^\circ$. We have also included here the second Born results of Vucic *et al.*

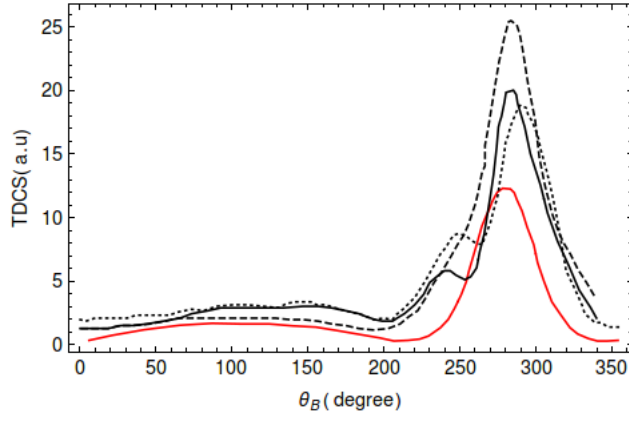


Figure 2: The TDCS of the $(e, 2e)$ ionization of hydrogen 2S in terms of the ejection angle θ_B . The incident and the ejected electron kinetic energies are 250 eV and 5 eV respectively and the scattering angle $\theta_f = 5^\circ$. The solid red line gives our results (NRCBA) given in (53), the solid black line those of Hafid *et al.* [5], the dotted line those of Vucic *et al.* [6] and the dashed line results obtained using Coulomb wave functions.

and it is clearly seen, from this figure for $\theta_f = 5^\circ$, that there is an apparent differences between the results obtained from the various calculations. The binary peak value of the present calculation is lowest among all calculations and is about half of that which uses Coulomb wave functions. In the recoil region, all results remain close in form and magnitude. It is interesting to see that the results of Hafid *et al.* reveal a peak which is present also in the second Born calculation of Vucic *et al.* and absent in the other calculations, where the Coulomb wave functions are used. Comparing Figs. (1) and (2), we note that the magnitude of the two peaks decreases with increasing the scattering angle θ_f . We study in Fig. (3), for the same kinetic energy, the variation of the NRCBA in terms of the scattering angle θ_f for the ejection angle $\theta_B = 20^\circ$. The comparison with the results of Hafid *et al.* is also included. This actually gives a sharp peak, higher than the other peaks in the previous figures. We observe also that the scattered electron, which is relatively faster than the ejected one, goes out with small angles. Figure (4) depicts the TDCS in the SRCBA and the corresponding one in the NRCBA for the scattering angle $\theta_f = 3^\circ$. The incident electron kinetic energy is $T_i = 250$ eV and the ejected electron kinetic energy is $T_B = 5$ eV. We see that the two curves are identical and have two peaks, one in the interval between -180° and 0° (recoil peak) and the other in the range between 0° and 180° (binary peak). However, even in the nonrelativistic regime, small effects are presented; due to the semirelativistic treatment of the wave functions that we have used in the SRCBA, and these can only be related to the spin effect.

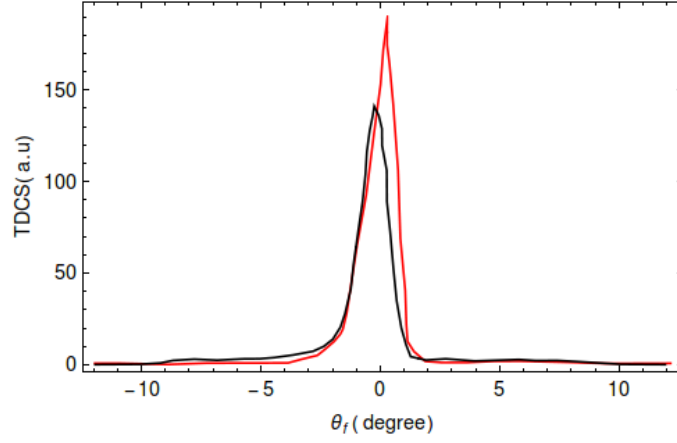


Figure 3: The TDCS of the (e, 2e) ionization of hydrogen 2S in terms of the scattering angle θ_f . The incident and the ejected electron kinetic energies are 250 eV and 5 eV respectively and the ejection angle $\theta_B = 20^\circ$. The solid red line gives our results (NRCBA) given in (53) and the solid black line those of Hafid *et al.* [5]

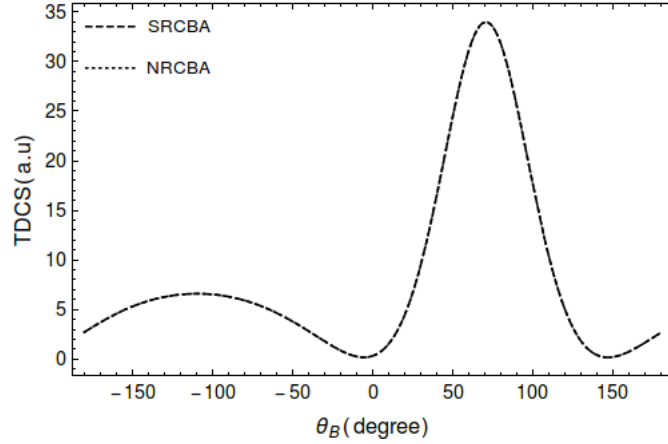


Figure 4: The two TDCSs as a function of the ejection angle θ_B . The incident and the ejected electron kinetic energies are 250 eV and 5 eV respectively and the scattering angle $\theta_f = 3^\circ$. The other angles are chosen as follows: $\theta_i = 0^\circ$, $\phi_i = 0^\circ$, $\phi_f = 0^\circ$ and $\phi_B = 180^\circ$.

B. Symmetric coplanar geometry

In symmetric geometry, as we mentioned previously, the kinetic energies of both scattered and ejected electrons are required to be approximately equal. The TDCS, in all models studied in the previous section, depends explicitly on the kinetic energy values of the scattered and ejected electrons, in addition to the different spherical coordinates related to each electron. Therefore, care must be taken when choosing the values of these kinetic energies, so that the above-mentioned

geometry condition is fulfilled. We remind the reader here of the relation that allows us to obtain these values without violating the requirement of symmetric geometry. Using the kinetic energy conservation $T_f = T_i + \varepsilon_{2S} - T_B$, we find that, according to the condition $T_f = T_B$, $T_B = (T_i + \varepsilon_{2S})/2$, where $\varepsilon_{2S} = -3.4 \text{ eV} = -0.125 \text{ a.u.}$ is the nonrelativistic binding energy of atomic hydrogen in its metastable 2S-state. Thus, every kinetic energy of the incoming electron corresponds to a kinetic energy of the scattered electron determined from that relation so that the condition of symmetric geometry always remains true. For the symmetric coplanar geometry, we choose the following angular situation where p_i is along the z -axis ($\theta_i = 0^\circ, \phi_i = 0^\circ$). For the scattered electron, we choose ($\theta_f = 45^\circ, \phi_f = 0^\circ$) and for the ejected electron we choose $\phi_B = 180^\circ$ and the angle θ_B varies differently from a figure to another. First of all, we will try to clarify the limit between the relativistic and non-relativistic domains in the case of the ionization of the hydrogen atom from its metastable 2S-state. Because, compared to the results of the ground state, we found that there is a significant difference between the two non-relativistic limit values. If the hydrogen atom is ionized from its ground 1S-state, the non-relativistic limit value is defined by the relativistic parameter ($\gamma = [1 - (\beta/c)^2]^{-1/2}$) value of 1.0053 which corresponds to an incident electron kinetic energy of 2700 eV. We recall here that, in atomic units, the kinetic energy is related to γ parameter by the following relation: $T_i = c^2(\gamma - 1)$. It means that when the value of the relativistic parameter γ is greater than 1.0053, a difference between the relativistic and non-relativistic kinetic energies will appear. In the case of the ionization of the hydrogen atom from its metastable 2S-state, we found that the non-relativistic limit changed and increased slightly from 2700 eV until it reached the value of 4250 eV. In Fig. (5), it can be seen that there is no difference at all between the TDCSs (RPWBA, SRPWBA and NRPWBA) in the non-relativistic limit, since all the curves of the three TDCSs are almost equal and identical. This figure represents the first check of our models in particular in the non-relativistic limit ($T_i = 4250 \text{ eV}$, $T_f = T_B = 2123.3 \text{ eV}$). But, we note that when we pass this limit by raising the kinetic energy of the incoming electron to 10 keV and 20 keV, the non-relativistic TDCS begins to differ from the other two TDCSs that remain equal as depicted in Fig. (6). Thus, the agreement between the relativistic and nonrelativistic models is good from the nonrelativistic limit and below ($T_i \leq 4250 \text{ eV}$), but the disagreement increases at high energies. It appears from Fig. (6) that at the relativistic domain, the effects of the spin terms and the relativity begin to be noticeable and that the non-relativistic formalism is no longer valid. We notice from Fig. (5) that there is a parfait symmetry around the value $\theta_B = 45^\circ$ and the three TDCSs are all peaked in the vicinity of the same value. We also note

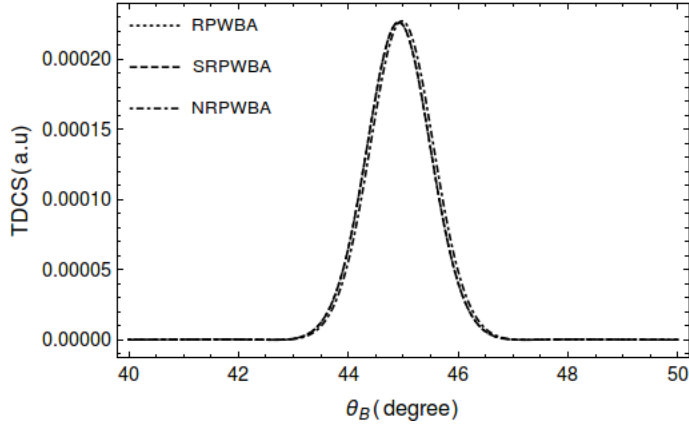


Figure 5: The Three TDCSs of the (e, 2e) ionization of hydrogen 2S as a function of the ejection angle θ_B . The incident and the ejected electron kinetic energies are 4250 eV and 2123.3 eV respectively and the scattering angle $\theta_f = 45^\circ$.

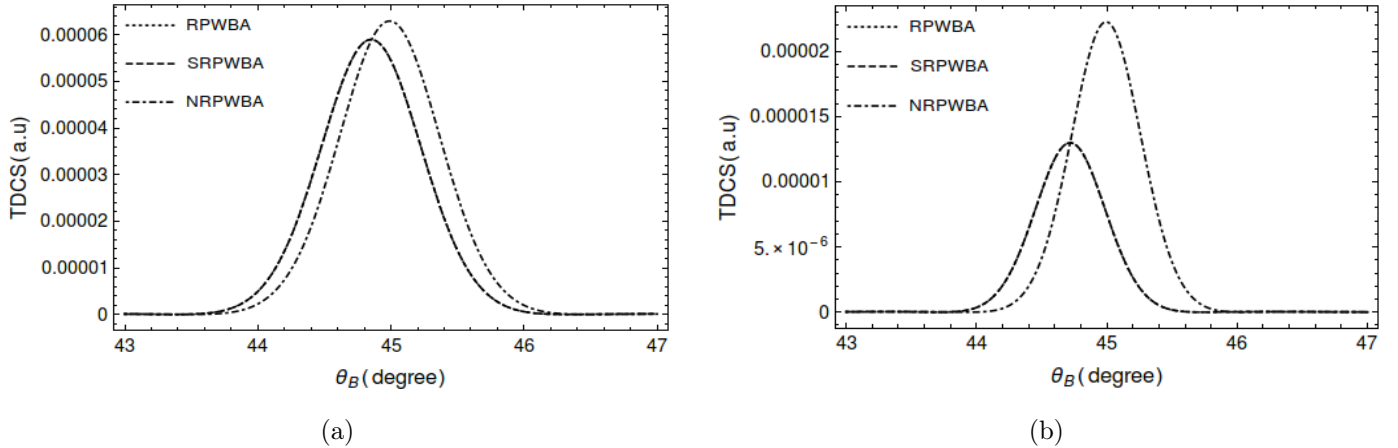


Figure 6: Same as in Fig. (5) but for the incident and the ejected electron kinetic energies of (a) 10000 eV and 4998.3 eV and (b) 20000 eV and 9998.3 eV respectively.

from Fig. (6) that the binary peak position in the relativistic domain begins with a shift towards smaller values than 45° . Comparing Figs. (5) and (6), it is clearly seen that the magnitude of the binary peak decreases with increasing the kinetic energy of the incident electron, which is the usual behavior in charged particle-impact ionization of an atom. By the way, these two relativistic and semirelativistic TDCSs (RPWBA and SRPWBA) remain the same and equal, regardless of the kinetic energy value of the incoming electron. For example, we give in Fig. (7) a representation of the RPWBA and SRPWBA at high incident kinetic energy of 511002 eV. It appears to us through

Fig. (7) that the two TDCSs (RPWBA and SRPWBA), despite the different wave functions used to describe the hydrogen atom in each of them, give the same results even at high energies. This fact was proven and applied in more than one place when studying the excitation or ionization of the hydrogen atom where it is sufficient to use only the Darwin wave function, instead of the exact analytical wave function, as a semirelativistic state to represent the atomic hydrogen, and it was found that this gives nearly the same results as the exact description only when the condition $Z\alpha \ll 1$ is fulfilled. This is precisely the reason why, when studying theoretically asymmetric geometry in the previous section, we were satisfied with only the treatment of the SRCBA model without the corresponding one in the Relativistic Coulomb Born Approximation (RCBA), so there is no need to complicate the calculation more as long as both give the same results. For the sake of

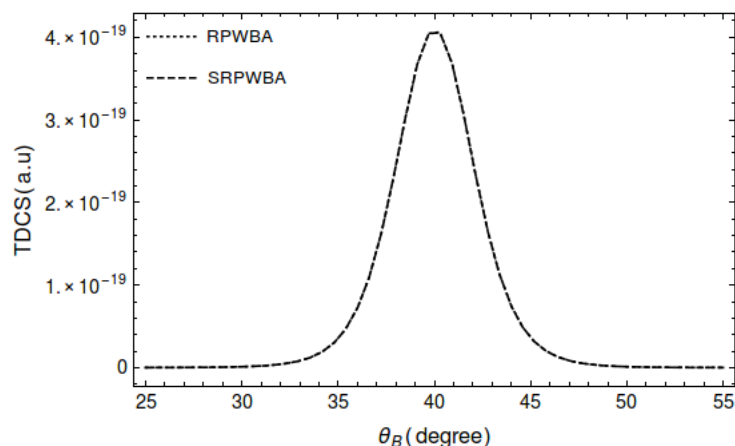


Figure 7: The two TDCSs in the relativistic regime as a function of the ejection angle θ_B . The incident and the ejected electron kinetic energies are 511002 eV and 255499.3 eV respectively and the scattering angle $\theta_f = 45^\circ$.

illustration, in a similar way to the 2D-plot, the contour plot in Fig. (8) exhibits more informations on the variation and the shape of the TDCS in the RPWBA versus both incident electron kinetic energy and angle θ_B in the binary coplanar geometry. For the variation with respect to θ_B , we observe that the TDCS decreases at small and large angles. We see also that the TDCS presents a maximum only at the particular point of $\theta_B = \theta_f = 45^\circ$, and its magnitude at this particular point decreases as the electron kinetic energy increases. Figure (9) shows that when the incident electron kinetic energy increases provided that $\theta_B = \theta_f = 45^\circ$, the peak of the TDCS decreases and remains nearly around $\phi_B = 180^\circ$. From Fig. (9), we see that as the energy increases, the probability to observe the ejected electron in the direction $\phi_B = 180^\circ$ diminishes progressively.

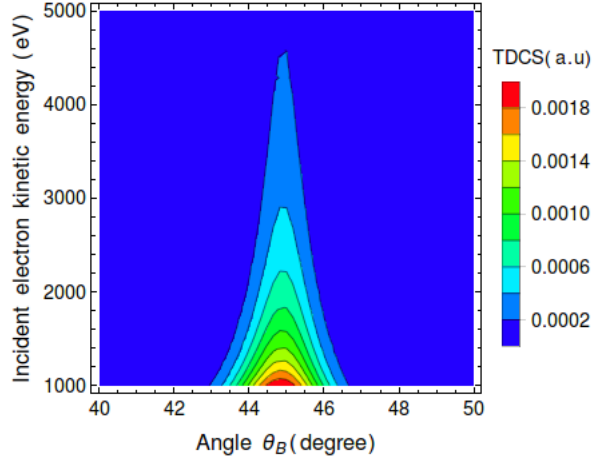


Figure 8: The TDCS, in RPWBA, as a function of the angle θ_B of the ejected electron and the incident electron kinetic energy T_i varying from 1000 eV to 5000 eV. We have used the condition

$$40^\circ \leq \theta_f = \theta_B \leq 50^\circ.$$

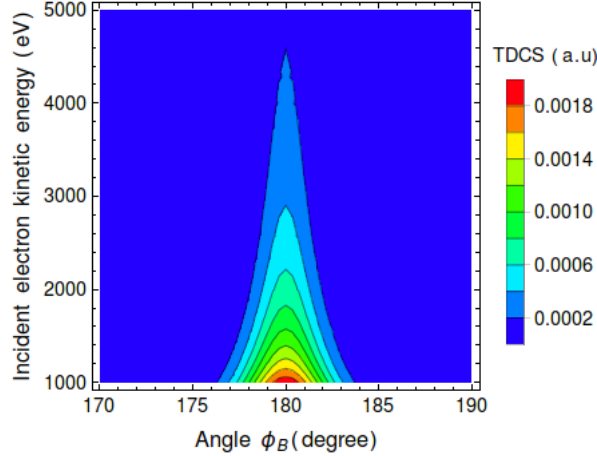


Figure 9: The TDCS, in RPWBA, as a function of the angle ϕ_B of the ejected electron and the incident electron kinetic energy T_i varying from 1000 eV to 5000 eV for $\theta_B = \theta_f = 45^\circ$.

Figure (9) also shows that for all figures in the symmetric geometry, in which we choose ϕ_B to be constant, it must be equal to 180° since the pick is clearly located at the same value. Figure (10) represents the variations of TDCS in the RPWBA in terms of the scattered and ejected electron angles at the energies $T_i = 5000$ eV and $T_B = 2498.3$ eV. The purpose of including this figure is to show how important the condition on both angles to be verified in the symmetric coplanar geometry. Through this figure, it becomes clear to us that the TDCS represents a maximum value at $\theta_f = \theta_B = 45^\circ$ and begins to decrease directly in the areas where this condition is broken. From

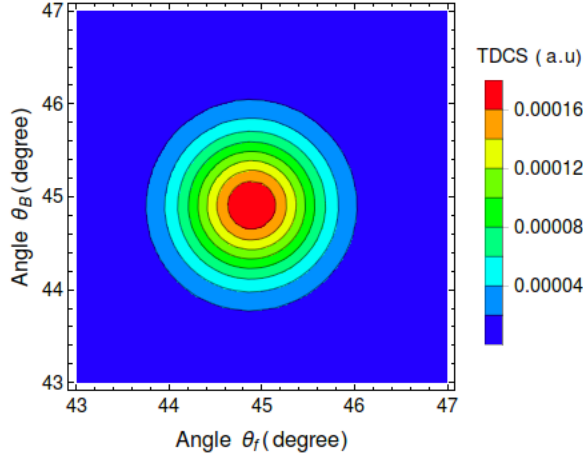


Figure 10: The TDCS, in RPWBA, as a function of the angle θ_B of the ejected electron and the angle θ_f of the scattered electron for $T_i = 5000$ eV and $T_B = 2498.3$ eV.

here it becomes evident that we must always respect this requirement and take it into account when working within the symmetric coplanar geometry. In Fig. (11), we plot the two TDCSs (SRCBA and NRCBA) with respect to the symmetric coplanar geometry at relativistic energies. In the relativistic regime, by increasing the value of the incident kinetic energy (10 keV, 15 keV, 20 keV), we notice the shift of the maximum of the TDCS in the SRCBA towards smaller values than $\theta_B = 45^\circ$, as well as the fact that the SRCBA is always lower than the NRCBA. Recall that in the non-relativistic domain, we have already compared our results for the two asymmetric and symmetric coplanar geometries. In Fig. (12), we plot the RPWBA and the NRPWBA with the two TDCSs (SRCBA and NRCBA). We see that the NRCBA and the SRCBA are the same and they give a lower TDCS due to the fact that the ejected electron still feels Coulomb effect of the residual ion as much as its kinetic energy ($T_B = 123.3$ eV in this case) is insufficient to cross the Coulomb barrier imposed by the residual ion. By increasing the kinetic energy of the incident and ejected electrons simultaneously (always checking the symmetric coplanar geometry), we find that the ejected electron begins slowly to escape from the Coulomb effect until it completely crosses it at kinetic energy $T_B = 1623.3$ eV. In Fig. (12b), there is a very good agreement between the four models and they produce the same results as the use of the Coulomb wave function is no longer necessary.

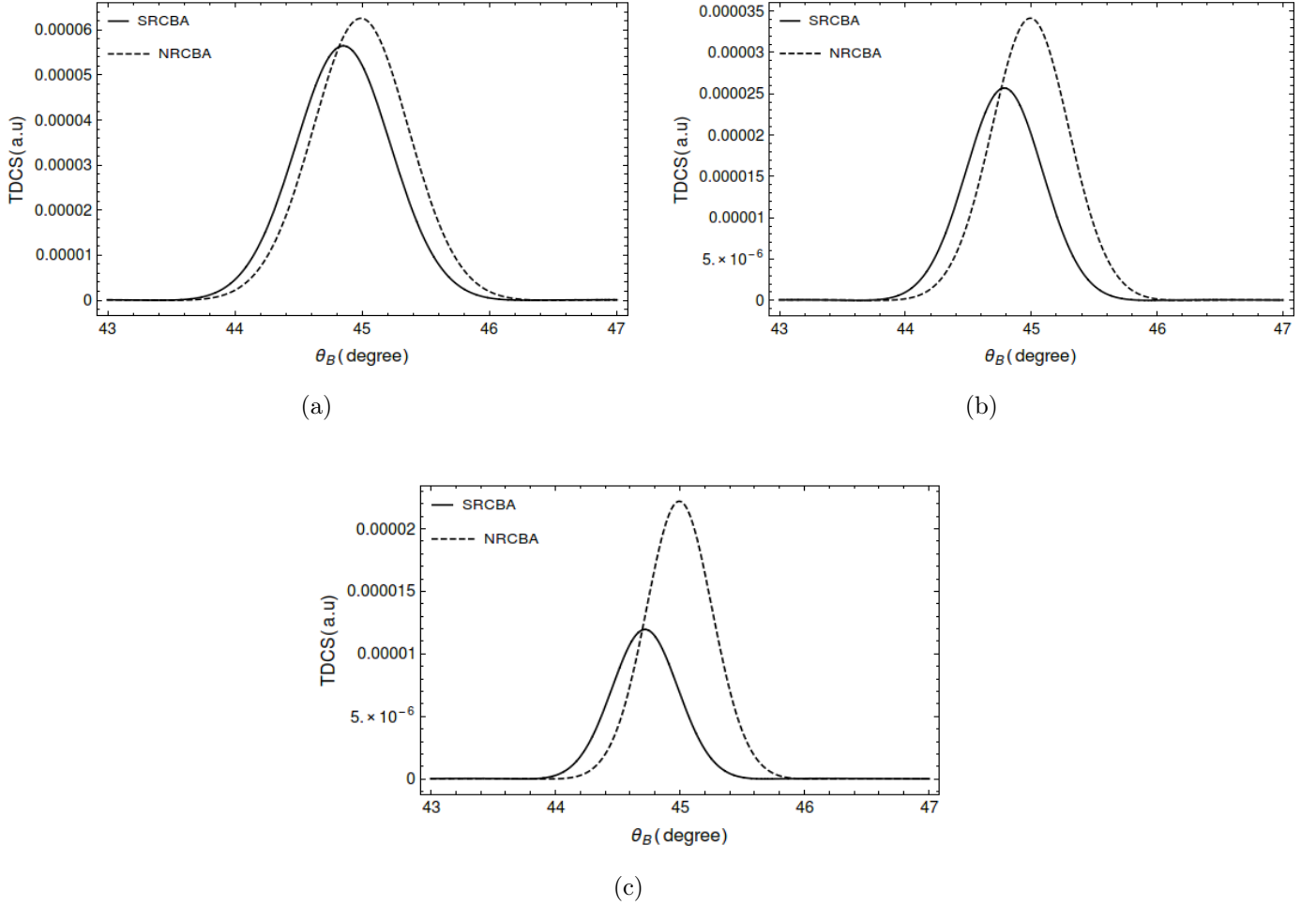


Figure 11: The two TDCSs in symmetric coplanar geometry as a function of the ejection angle θ_B for the scattering angle $\theta_f = 45^\circ$. The incident and the ejected electron kinetic energies are (a) $T_i = 10000$ eV and $T_B = 4998.3$ eV, (b) $T_i = 15000$ eV and $T_B = 7498.3$ eV and (c) $T_i = 20000$ eV and $T_B = 9998.3$ eV.

IV. CONCLUSION

In this work, we have calculated the triple differential cross sections (TDCS) for the ionization of hydrogen atom by electrons impact in the metastable 2S-state for asymmetric and symmetric coplanar geometries. In the asymmetric coplanar geometry, we have compared our nonrelativistic results with those of other theories and found that the present model is close to that obtained by Coulomb wave functions only at the scattering angle $\theta_f = 3^\circ$. Outside this value, there is significant difference between the different theoretical approaches in which the present results being the minimum. In the symmetric coplanar geometry, a new nonrelativistic limit value is

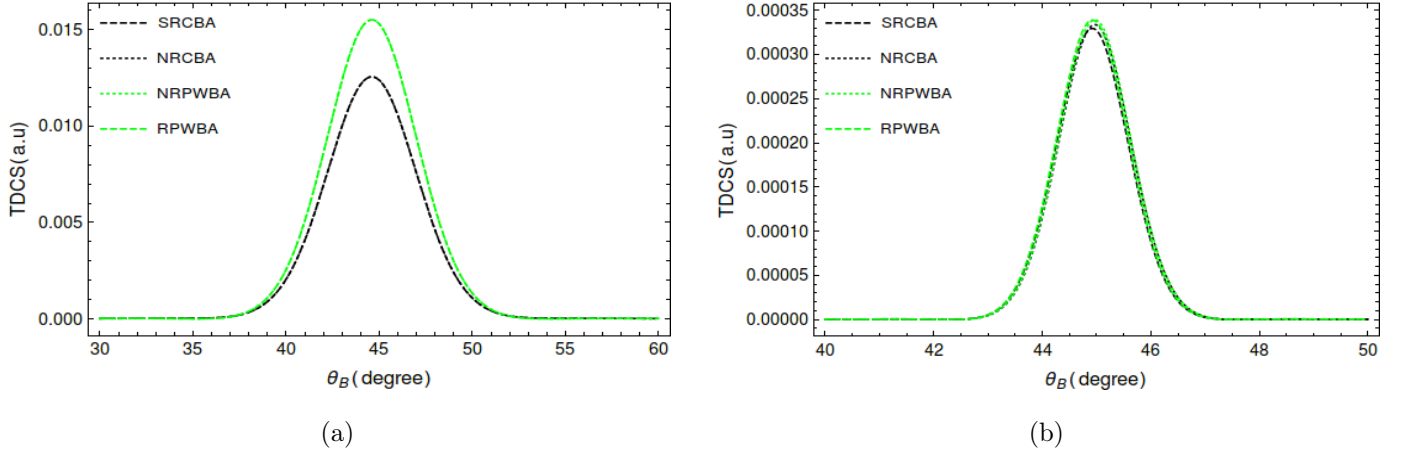


Figure 12: The four TDCSs in symmetric coplanar geometry as a function of the ejection angle θ_B for the scattering angle $\theta_f = 45^\circ$. The incident and the ejected electron kinetic energies are
(a) $T_i = 250$ eV and $T_B = 123.3$ eV and (b) $T_i = 3250$ eV and $T_B = 1623.3$ eV.

determined theoretically to be 4250 eV, which is very different from that known for the ground state (2700 eV). Relativistic triple differential cross section have been evaluated within the relativistic model (RPWBA) in the first Born approximation. The consistency of this theoretical model is checked by taking the nonrelativistic limit. Semirelativistic TDCS in the SRPWBA gives nearly the same results, regardless of the kinetic energy of the incoming electron, as the RPWBA if the condition $Z\alpha \ll 1$ is satisfied. It is shown that the nonrelativistic formalism is no longer valid, in both geometries, for incident kinetic energies higher than 10 keV, due to the spin and relativistic effects which begin to appear at high energies. Comparing our results for the two asymmetric and symmetric coplanar geometries, we found that the use of the Coulomb wave function to describe the ejected electron is no longer necessary as long as its kinetic energy $T_B \geq 1623.3$ eV. The validation of this work requires an experimental study. We hope that our results should serve as a motivation to perform such collisions experiments in the future.

-
- [1] H. Ehrhardt, M. Schulz, T. Tekaet, and K. Willmann, Phys. Rev. Lett. **22**, 89 (1969).
 - [2] U. Amaldi, A. Egidi, R. Marconero, and G. Pizzella, Rev. Sci. Instrum. **40**, 1001 (1969).
 - [3] A. J. Dixon, A. Von Engel, and M. F. A. Harrison, Proc. R. Soc. Lond. A. **343**, 333 (1975).
 - [4] P. Defrance, W. Clays, A. Cornet, and G. Poulaert, J. Phys. B: At. Mol. Phys. **14**, 111 (1981).

- [5] H. Hafid, B. Joulakian, and C. Dal Cappello, J. Phys. B **26**, 3415 (1993).
- [6] S. Vučić, R. M. Potvliege, and C. J. Joachain, Phys. Rev. A **35**, 1446 (1987).
- [7] M. Brauner, J. S. Briggs, and H. Klar, J. Phys. B: At. Mol. Opt. Phys. **22**, 2265 (1989).
- [8] S. Dhar, Aust. J. Phys. **49**, 937 (1996).
- [9] J. N. Das and S. Dhar, Pramana J. Phys. **47**, 263 (1996).
- [10] R. Biswas and C. Sinha, Nuovo Cimento D **16**, 571 (1994).
- [11] H. Ray and A. C. Roy, J. Phys. B: At. Mol. Opt. Phys. **21**, 3243 (1988).
- [12] J. Eichler and W. E. Meyerhof, *Relativistic Atomic Collisions* (Academic, New York, 1995).
- [13] H. S. W. Massey and C. B. O Mohr, Proc. R. Soc. London **140**, 613 (1933).
- [14] M. S. Gravielle and J. E. Miraglia, Computer Physics Communications **69**, 53 (1992).
- [15] Y. Attaourti, S. Taj, and B. Manaut, Phys. Rev. A **71**, 062705 (2005).
- [16] W. Greiner and J. Reinhardt, *Quantum Electrodynamics* (Springer-Verlag, Berlin, 1992).
- [17] C. J. Joachain, *Quantum Collision Theory*, (Edition North-Holland Publishing Company Amsterdam, 1975).